3-2014

Resonant scattering of energetic electrons by unusual low-frequency hiss

Binbin Ni
University of California - Los Angeles

Wen Li
University of California - Los Angeles

R. M. Thorne
University of California - Los Angeles

J. Bortnik
University of California - Los Angeles

Qianli Ma
University of California - Los Angeles

See next page for additional authors

Recommended Citation
Ni, B., et al. (2014), Resonant scattering of energetic electrons by unusual low-frequency hiss, Geophys. Res. Lett., 41, 1854–1861, doi:10.1002/2014GL059389.

AGU PUBLICATIONS

Geophysical Research Letters

RESEARCH LETTER
10.1002/2014GL059389

Key Points:
- Unusual hiss scatters ~50-200 keV electrons more rapidly than normal hiss
- Resultant electron lifetimes can be of ≤ 1 hour for energetic electrons
- Unusual hiss scattering should be incorporated into radiation belt modeling

Correspondence to:
B. Ni,
bbni@atmos.ucla.edu

Citation:
Ni, B., et al. (2014), Resonant scattering of energetic electrons by unusual low-frequency hiss, *Geophys. Res. Lett.*, *41*, 1854–1861, doi:10.1002/2014GL059389.

Received 22 JAN 2014
Accepted 4 FEB 2014
Accepted article online 6 FEB 2014
Published online 27 MAR 2014

Resonant scattering of energetic electrons by unusual low-frequency hiss

Binbin Ni[1], Wen Li[1], Richard M. Thorne[1], Jacob Bortnik[1], Qianli Ma[1], Lunjin Chen[2], Craig A. Kletzing[3], William S. Kurth[3], George B. Hospodarsky[3], Geoffrey D. Reeves[4], Harlan E. Spence[5], J. Bernard Blake[6], Joseph F. Fennell[6], and Seth G. Claudepierre[6]

[1]Department of Atmospheric and Oceanic Sciences, UCLA, Los Angeles, California, USA, [2]Physics Department, University of Texas at Dallas, Richardson, Texas, USA, [3]Department of Physics and Astronomy, University of Iowa, Iowa City, Iowa, USA, [4]Space Science and Applications Group, Los Alamos National Laboratory, Los Alamos, New Mexico, USA, [5]Institute for the Study of Earth, Oceans, and Space, University of New Hampshire, Durham, New Hampshire, USA, [6]The Aerospace Corporation, Los Angeles, California, USA

Abstract We quantify the resonant scattering effects of the unusual low-frequency dawnside plasmaspheric hiss observed on 30 September 2012 by the Van Allen Probes. In contrast to normal (~100–2000 Hz) hiss emissions, this unusual hiss event contained most of its wave power at ~20–200 Hz. Compared to the scattering by normal hiss, the unusual hiss scattering speeds up the loss of ~50–200 keV electrons and produces more pronounced pancake distributions of ~50–100 keV electrons. It is demonstrated that such unusual low-frequency hiss, even with a duration of a couple of hours, plays a particularly important role in the decay and loss process of energetic electrons, resulting in shorter electron lifetimes for ~50–400 keV electrons than normal hiss, and should be carefully incorporated into global modeling of radiation belt electron dynamics during periods of intense injections.

1. Introduction

Plasmaspheric hiss is an important magnetospheric emission responsible for inner magnetospheric electron precipitation over a broad energy range. Hiss-induced relativistic electron precipitation loss accounts for the formation of the slot region between the inner and outer radiation belts [*Lyons and Thorne*, 1973]. Hiss scattering also plays an important role in driving the slow decay of outer zone relativistic electrons (1–10 MeV) on time scales of tens to hundreds of days and more rapid loss of <1 MeV electrons with time scales of days or less [e.g., *Meredith et al.*, 2006, 2007; *Summers et al.*, 2007, 2008; *Thorne et al.*, 2013; *Ni et al.*, 2013]. The hiss wave normal distribution is primarily quasi-parallel near the geomagnetic equator and becomes more oblique when propagating to higher latitudes [e.g., *Santolík et al.*, 2001; *Agapitov et al.*, 2012], and the dominant wave power typically occurs over a band between 100 Hz and 2 kHz with a spectral intensity peak at several hundred hertz [e.g., *Meredith et al.*, 2006, 2007, 2009; *Summers et al.*, 2008], which is commonly adopted in models to quantify the resonant scattering of radiation belt electrons [e.g., *Meredith et al.*, 2006, 2007, 2009; *Summers et al.*, 2007; *Thorne et al.*, 2013; *Ni et al.*, 2013].

Recently, *Li et al.* [2013] reported an unusual enhancement of plasmaspheric hiss observed by the Electric and Magnetic Field Instrument Suite and Integrated Science (EMFISIS) instrument [*Kletzing et al.*, 2013] on board the Van Allen Probes [*Mauk et al.*, 2013] on 30 September 2012, which exhibited a frequency spectrum extending as low as ~ 20 Hz, with ~90% of the wave power below ~100 Hz. The observations also indicated that these unusually low-frequency hiss emissions were excited for a few hours by localized cyclotron resonance instability in the dawnside outer plasmasphere following convective injection of plasma sheet electrons into the plasmasphere. Here we adopt a realistic model for the unusual hiss and investigate its role in resonant scattering of radiation belt energetic electrons and the resultant dynamical evolution of the electron pitch angle distribution.

2. Unusual Hiss Observations and Model Development

The EMFISIS observations on board the Van Allen Probe A of the unusual intense hiss emissions on 30 September 2012 are shown in Figure 1 for the period of 15–19 UT. Enhanced broadband electromagnetic hiss

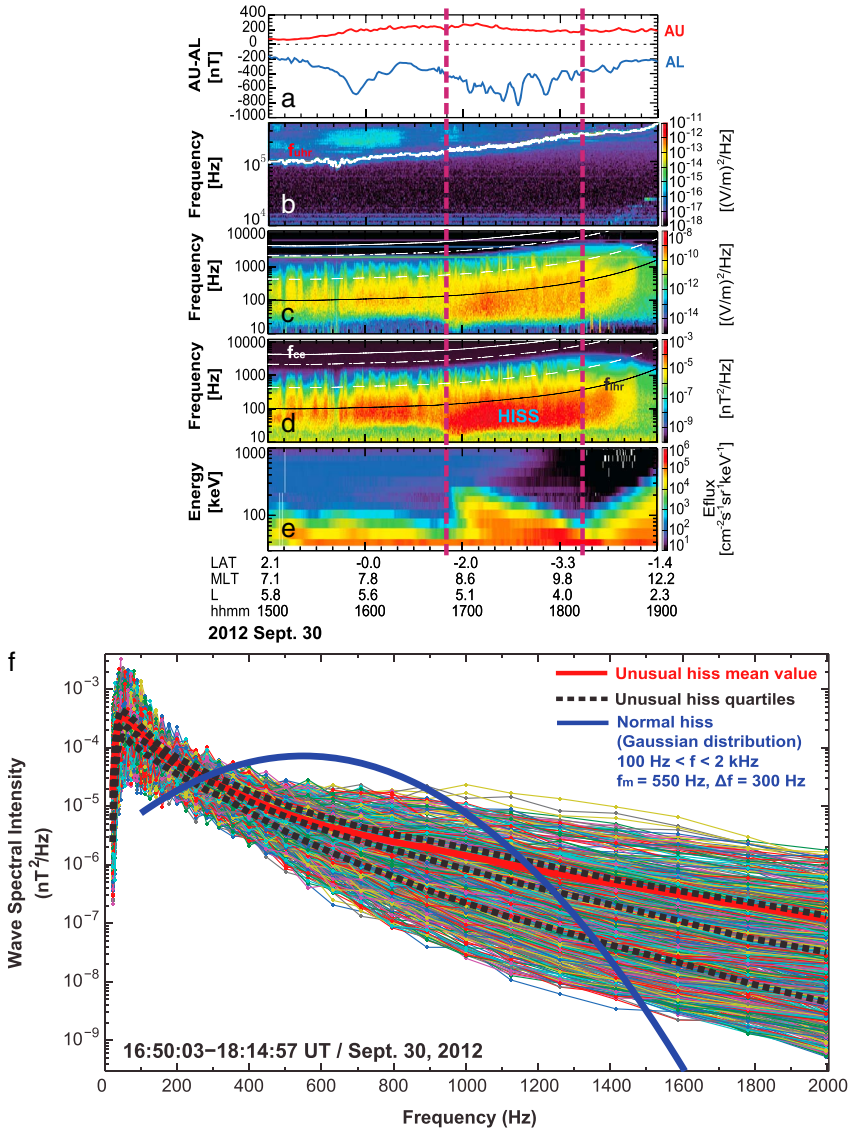

Figure 1. (a) *AU* and *AL* indices, (b) frequency time spectrogram of electric field spectral density in the EMFISIS high-frequency receiver channel with the overplotted upper hybrid resonance frequency line (f_{uhr}, white curve), (c and d) frequency time spectrogram of electric and magnetic field spectral density in the EMFISIS waveform receiver channel, and (e) energy spectrogram of spin-averaged electron flux measured by MagEIS on board the Van Allen Probe A during the period of 15–19 UT on 30 September 2012. In Figures 1c and 1d, the overplotted white lines represent f_{ce} (solid), 0.5 f_{ce} (dash dotted), and 0.1 f_{ce} (dashed), and the black line indicates f_{lhr}, where f_{ce} is equatorial electron cyclotron frequency and f_{lhr} is lower hybrid resonance frequency. (b) Line plots of unusual low-frequency hiss spectral intensities of magnetic fields during 16:50:03–18:14:57 UT, together with the mean profile (thick red), the quartiles (dotted thick black), and the Gaussian spectrum for normal hiss with the same integrated wave amplitude (thick blue).

waves [*Li et al.*, 2013] occurred at frequencies > ~40 Hz to ~2 kHz for the first 2 h starting at 15 UT. Corresponding to the dramatic flux increase of ~50–200 keV electrons measured by the Magnetic Electron Ion Spectrometer (MagEIS) instrument [*Blake et al.*, 2013] at ~16:50 UT, the plasmaspheric hiss extended to lower frequencies, down to ~20 Hz with further intensification, and was observed continuously for more than 1 h until the satellite moved to lower altitudes of $L <$ ~3. The upper hybrid frequency (f_{uhr}) line was identified by the EMFISIS high-frequency receiver channel and is shown as white curve in Figure 1b. Of particular interest to our study is the time interval of 16:50–18:15 UT when Probe A crossed the region of $L = 3.7$–5.3 at 8.5–10 magnetic local time (MLT) and observed the most intense hiss emissions with wave amplitudes (B_W) integrated over 20–2000 Hz well above 100 pT. The

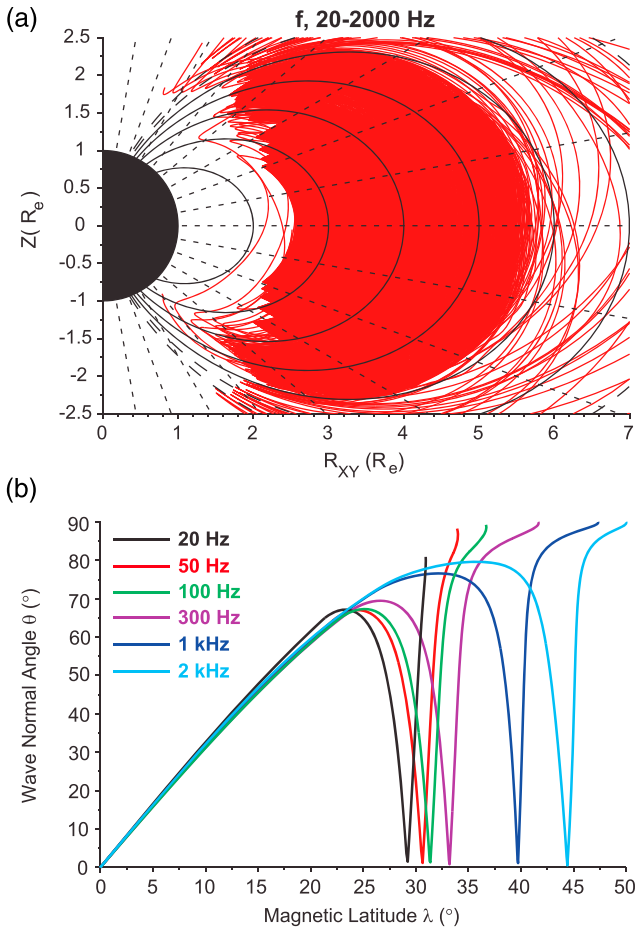

Figure 2. (a) Raypaths in the plane of (R_{XY} (= $\sqrt{x^2+y^2}$), Z) and propagation characteristics of 20–2000Hz (in steps of 10 Hz) hiss waves launched at the equatorial location $L = 5$. (b) Corresponding latitudinal variations of hiss wave normal angles for representative frequencies of 20 Hz, 50 Hz, 100 Hz, 300 Hz, 1 kHz, and 2 kHz.

ambient plasma density (N_e) inferred from the spacecraft potential and the upper hybrid line increased from ~300 cm^{-3} to ~900 cm^{-3}.

The EMFISIS spectral intensity data for the 75 min time interval are shown in Figure 1f. While there were large variations in wave spectral intensity above 1 kHz, the hiss wave intensity peaked at frequencies ~50 Hz and the majority of the wave power was confined below 200 Hz. The quartiles of the spectral intensity data are shown as the thick dashed black curves, and the mean value, shown as the thick solid red curve, yields an average integrated hiss amplitude of 195 pT. For comparison, the thick solid blue curve shows the spectral intensity of normal hiss with the same amplitude but characterized by a nominal Gaussian frequency spectrum in terms of $\exp\left[-\left(\frac{f-f_m}{\Delta f}\right)^2\right]$ with the peak wave frequency f_m = 550 Hz, the frequency width Δf = 300 Hz, the lower cutoff frequency f_{lc} = 100 Hz, and the upper cutoff frequency f_{uc} = 2 kHz [e.g., *Meredith et al.*, 2006; *Summers et al.*, 2007; *Thorne et al.*, 2013]. The normal hiss has larger spectral intensities at frequencies of 300–1200 Hz, but the unusual hiss is much stronger at frequencies $<$ 200 Hz. At frequencies $>$ 1200 Hz, the wave intensity of the unusual hiss is also stronger than normal hiss.

The distribution of wave normal angle as a function of latitude is another critical parameter required for reliable quantification of hiss-induced scattering rates, which cannot be directly obtained from observations for this event. To acquire this information, ray tracing simulations were performed [e.g., *Chen et al.*, 2012] with a postdawn plasmapause between $L = 5.5$ and $L = 5.8$. A diffusive equilibrium density model [*Bortnik et al.*, 2011] is used, with the equatorial density profile fitted by the plasma density derived from the EMFISIS observed upper hybrid line (Figure 1). Waves with frequencies between 20 Hz and 2 kHz (in steps of 10 Hz) were launched along the field line at the magnetic equator at $L = 5$, and the resulting raypaths are shown in Figure 2a, illustrating the propagation characteristics of hiss emissions at various frequencies inside the plasmasphere. The corresponding latitudinal variations of hiss wave normal angles are shown in Figure 2b. A secondary field-aligned component at high magnetic latitudes (~30°–40°) occurs near the inner edge of the plasmapause as a consequence of the refraction associated with the density gradient. Because the secondary component only occurred over a narrow L range near the inner edge of plasmapause and we are interested in a general trend of wave normal angle variation inside the plasmasphere of much larger L shell range, the field-aligned component is ignored for our wave normal angle model. It is evident that the maximum magnetic latitude of the hiss power is strongly frequency dependent, increasing from ~30° for 20 Hz to ~33° for 100 Hz to ~45° for 2 kHz. At the same time, the waves become increasingly oblique when propagating toward higher latitudes, i.e., field-aligned at the equator and approaching high wave normal angles $>$ 80° at the frequency-dependent maximum latitude. These ray tracing simulations are used to develop a model for

Table 1. Adopted Wave Normal Angle Distribution at Each of the Indicated Eight Magnetic Latitude Intervals for the Unusual Hiss Event, According to the Ray Tracing Results Shown in Figure 2b[a]

$\lvert\lambda\rvert$(°)	θ_m(°)	θ_w(°)	θ Range (°)
0–5	0	15	0–20
5–10	15	20	0–30
10–15	30	25	10–50
15–20	40	35	20–60
20–25	60	40	30–75
25–30	70	50	40–80
30–35	75	60	50–80
35–40	80	70	55–85

[a]Note that 20–100 Hz waves are confined to the magnetic latitudes of $\lvert\lambda\rvert \le 30°$ and 100–2000 Hz waves are confined to $\lvert\lambda\rvert \le 40°$.

the hiss latitudinal coverage and its wave normal angle. Specifically, we set the 20–100 Hz waves to be confined to magnetic latitudes of $\lvert\lambda\rvert \le 30°$ and the 100–2000 Hz components to be confined to $\lvert\lambda\rvert \le 40°$. In addition, a realistic model of the hiss wave normal angle distribution as a function of magnetic latitude is constructed based on Figure 2b, which is tabulated in Table 1. The wave normal angle distribution follows a Gaussian function of $\exp\left[-\left(\frac{\tan\theta-\tan\theta_m}{\tan\theta_w}\right)^2\right]$, where θ is the wave normal angle, θ_m is the peak wave normal angle, and θ_w is the angular width. Furthermore, the wave spectral intensities for both frequency groups are assumed unchanged within their respective latitudinal coverage, which is a good approximation based on the ray tracing simulations [*Chen et al.*, 2012].

3. Electron Scattering Rates and Resultant Pitch Angle Evolution

The University of California, Los Angeles (UCLA) Full Diffusion Code [*Ni et al.*, 2008; *Shprits and Ni*, 2009] is used to evaluate quasi-linear bounce-averaged diffusion coefficients of energetic electrons due to resonant interactions with broadband plasmaspheric hiss. We concentrate on the specific location at $L = 4.5$ and adopt a dipole geomagnetic field model. Based on the Van Allen Probes measurements, the average ambient electron density is 477 cm^{-3} for the period of 16:50–18:15 UT, producing a high ratio of equatorial electron plasma frequency to gyrofrequency of 21. Note that while during this time interval the severe erosion of the plasmapause was observed on the nightside with a compressed location down to well below 4 R_E [*Baker et al.*, 2013], the dayside plasmasphere was not eroded yet with a plasmapause location at > 5.5 R_E [*Li et al.*, 2013]. The diffusion rate computations for both the unusual hiss event and normal hiss include contributions from the $N = -10$ to $N = 10$ cyclotron harmonic resonances, including the Landau resonance $N = 0$. Taking into account the MLT constraint of such locally generated unusual hiss emissions, we apply an MLT-averaging factor of 1/8 by assuming that they were only present between 8 and 11 MLT. We note that to evaluate hiss-induced scattering rates, the hiss spectral intensity profile indicated by the thick solid red curve in Figure 1f is used (without any Gaussian fit) for the unusual hiss event, while the Gaussian spectrum indicated by the thick solid blue curve in Figure 1f is used for normal hiss. The total wave power for both wave spectra is the same with an integrated amplitude of 195 pT so that quantitative comparisons can be appropriately performed.

The drift- and bounce-averaged pitch angle scattering rates ($\langle D_{\alpha\alpha}\rangle$) are shown as a function of equatorial pitch angle (α_{eq}) and electron kinetic energy (E_k) in Figure 3a for normal hiss and in Figure 3b for the unusual hiss event. The drift- and bounce-averaged momentum diffusion rates (not shown) are very small for plasmaspheric hiss. Pronounced differences exist between the two computed $\langle D_{\alpha\alpha}\rangle$, and there are a number of interesting features to point out regarding the unusual low-frequency hiss scattering: (1) it can cause more efficient pitch angle scattering of $>$ ~50 keV electrons than normal hiss over a broad range of α_{eq} from high or intermediate pitch angles down to the loss cone (~4°), mainly due to the dominance of wave power at lower frequencies; (2) it can cause considerably decreased pitch angle scattering of $<$ 50 keV electrons at most pitch angles and of ~50 keV–2 MeV electrons at high pitch angles, mainly associated with decreased wave power at 300–1200 Hz that these electrons principally resonate with; and (3) it produces a narrower "bottleneck" (sharp drop in scattering rate at intermediate pitch angles) for electrons of 10 keV–~ 100 keV but a broader "bottleneck" for electrons of ~200 keV–2 MeV.

Line plots of $\langle D_{\alpha\alpha}\rangle$ shown in Figure 3c for the indicated five electron energies present more detailed variations of hiss scattering rate as a function of equatorial pitch angle and kinetic energy corresponding to the two cases of hiss emissions for quantitative comparisons. For 20 keV electrons, $\langle D_{\alpha\alpha}\rangle$ near the loss cone for the unusual hiss is reduced by a factor of over 3 compared to the normal hiss results. In contrast, for electrons of 100 keV and higher energies, $\langle D_{\alpha\alpha}\rangle$ near the loss cone for the unusual hiss emissions becomes

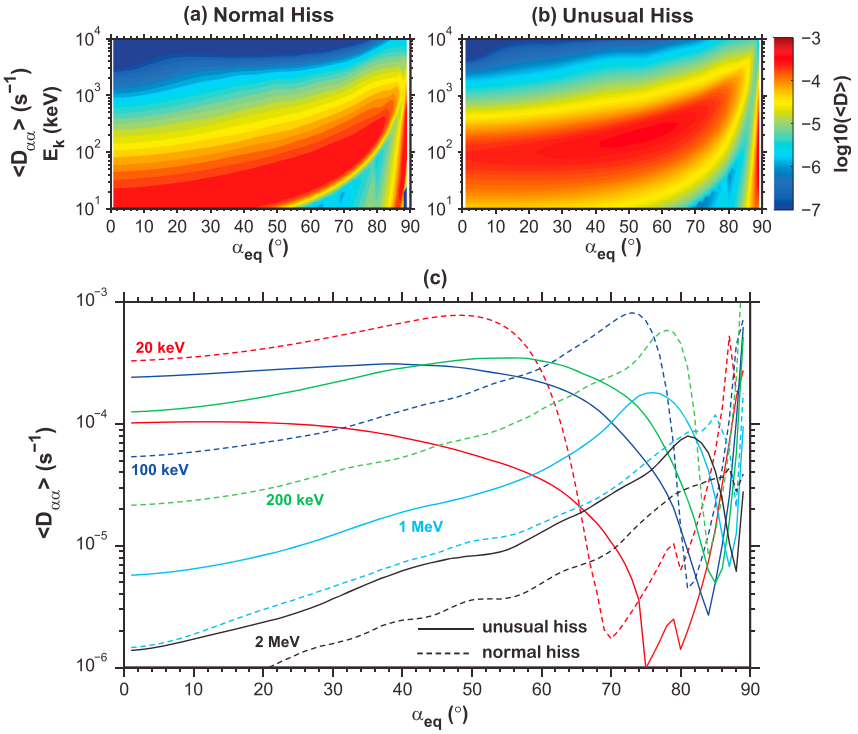

Figure 3. Two-dimensional plots of drift- and bounce-averaged pitch angle scattering rates $\langle D_{\alpha\alpha}\rangle$ as a function of electron kinetic energy E_k and equatorial pitch angle α_{eq} due to (a) normal hiss and (b) the unusual low-frequency hiss at $L = 4.5$. (c) Lines plots of $\langle D_{\alpha\alpha}\rangle$ as a function of α_{eq} for the indicated five electron energies due to normal hiss (dashed) and the unusual low-frequency hiss (solid).

larger by a factor of 3–6. The bottleneck becomes narrower for 20 keV electrons but broader for 200 keV–2 MeV electrons for the unusual hiss with decreased gradients in $\langle D_{\alpha\alpha}\rangle$. Besides the common feature that the bottleneck shifts to pitch angles closer to 90° as electron energy increases, the minimum $\langle D_{\alpha\alpha}\rangle$ also moves to higher α_{eq} for the unusual hiss event. Since $\langle D_{\alpha\alpha}\rangle$ at low pitch angles are very small for relativistic electrons ≥ 1 MeV and the observed unusual hiss only lasted for about 2 h, the net effect of the unusual hiss to scatter ≥ 1 MeV electrons is very likely to be negligible.

The pronounced differences in scattering rates between the unusual hiss event and normal hiss suggest that unusual hiss makes particular contributions to the dynamics of tens to hundreds keV energetic electrons, which we analyze subsequently using one-dimensional pure pitch angle diffusion simulations at a fixed L shell [e.g., *Meredith et al.*, 2009; *Thorne et al.*, 2013; *Ni et al.*, 2013]. We solve the equation

$$\frac{\partial f}{\partial t} = \frac{1}{T(\alpha_{eq})\sin(2\alpha_{eq})}\frac{\partial}{\partial \alpha_{eq}}\left[T(\alpha_{eq})\sin(2\alpha_{eq})\langle D_{\alpha\alpha}\rangle\frac{\partial f}{\partial \alpha_{eq}}\right], \quad (1)$$

where f is the phase space density (PSD), t is time, and the electron bounce period is approximated as $T(\alpha_{eq}) = 1.3802 - 0.3198\left(\sin(\alpha_{eq}) + \sqrt{\sin(\alpha_{eq})}\right)$ [*Lenchek et al.*, 1961]. The boundary conditions for PSD in α_{eq} space are $f(\alpha_{eq} \le \alpha_{LC}) = 0$ and $\frac{\partial f}{\partial \alpha_{eq}}(\alpha_{eq} = 90°) = 0$, where α_{LC} is equatorial bounce loss cone angle. By further assuming that the initial PSD follows a sinusoidal function of equatorial pitch angle, we model the temporal evolution of energetic electron pitch angle distribution due to the unusual hiss event and compare the results with those for the normal hiss case. Figure 4 shows the temporal changes of electron phase space density at five specified electron energies between 20 keV and 400 keV for a period of 2 h (the observed duration of the unusual hiss) corresponding to the cases of normal hiss and unusual hiss. The results are shown from the initial condition ($t = 0$) with an increment of 10 min to the state at $t = 2$ h, and the modeled PSDs are normalized to the initial PSD at $\alpha_{eq} = 90°$ so that all the values are ≤ 1.

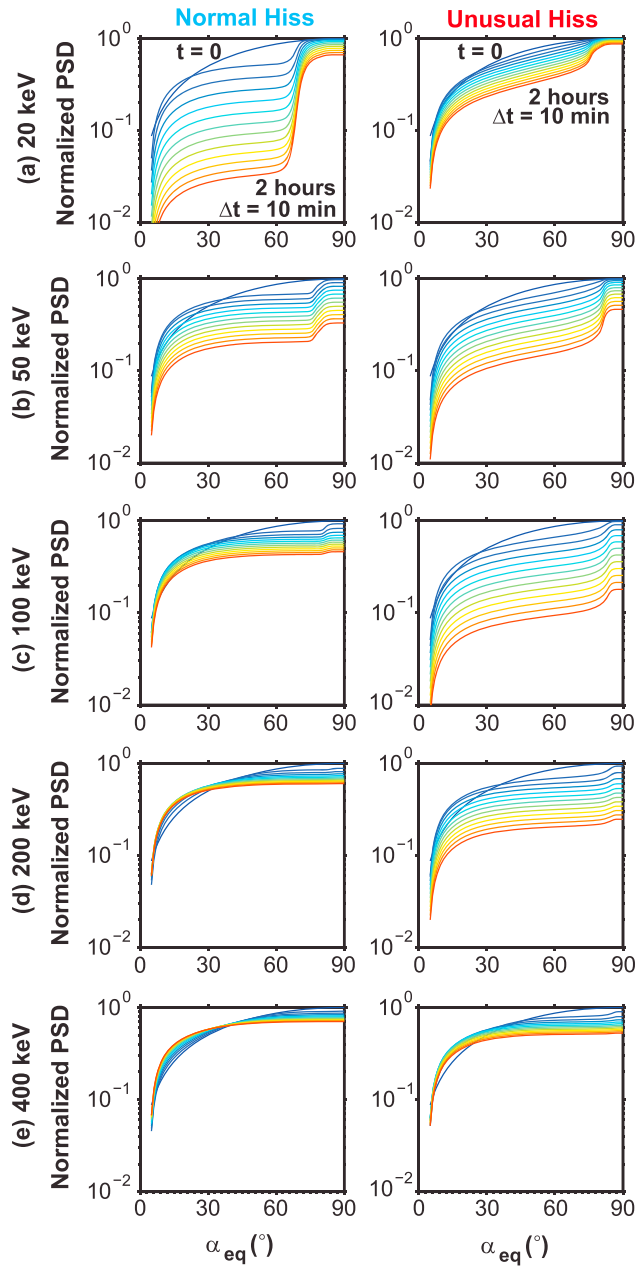

Figure 4. One-dimensional pitch angle diffusion simulation results of the pitch angle distribution for (a) 20 keV, (b) 50 keV, (c) 100 keV, (d) 200 keV, and (e) 400 keV electron phase space density (PSD) due to resonant scattering by (left) normal hiss and by (right) the unusual low-frequency hiss at $L = 4.5$. A time step of 1 s in real time is used during the entire 2 h simulation run for each energy, and the results are shown every 10 min. The modeled PSD is normalized to the initial PSD at $\alpha_{eq} = 90°$.

In accordance with the large differences in scattering rates for the two hiss cases, the modeled pitch angle evolution exhibits distinctly different features for radiation belt energetic electrons. Quantitative comparisons also indicated that normal hiss causes faster decay and loss of 20 keV electrons, but the unusual hiss event drives more rapid decay and loss of 50–200 keV electrons with the strongest removal occurring for 100 keV electrons within 2 h. The pancake pitch angle distribution [*Meredith et al.*, 1999] develops within tens of minutes for 20–100 keV electrons, which is more pronounced for the normal hiss scattering of 20–50 keV electrons and for the unusual hiss scattering of 50–100 keV electrons. We note that the top hat-shaped distribution due to the unusual hiss scattering is confined to larger pitch angles for 50–100 keV electrons. Overall, even though the wave duration was short (~ 2 h), the unusual hiss can significantly contribute to the pitch angle redistribution of

tens to hundreds keV electrons, leading to an electron temporal evolution substantially different from that driven by the 100–2000 Hz normal hiss. Scattering by the unusual hiss slows down the loss of 20 keV electrons but expedites the decay of 50–200 keV electrons. The resultant temporal evolution of the electron pitch angle distribution also represents a common two-step process that includes a relaxation from the initial condition toward the equilibrium state and a subsequent exponential decay as a whole (the lowest normal mode). Figure 4 indicates that the electron lifetimes due to scattering by the unusual low-frequency hiss can be of the order of 1 h for 50–200 keV electrons.

4. Conclusions and Discussion

Here we have performed a detailed investigation of the electron scattering effect of the unusual low-frequency hiss down to ~20 Hz observed by the Van Allen Probes on 30 September 2012. The drift- and bounce-averaged quasi-linear diffusion coefficients are evaluated for the unusual hiss event and are then adopted as inputs for one-dimensional diffusion simulations to model the evolution of the electron pitch angle distribution and the resultant time scales of relaxation toward equilibrium and subsequent overall decay under the lowest normal mode. Through quantitative comparisons with the results for normal hiss with a common Gaussian spectrum over 100–2000 Hz, the particular role of the unusual hiss in the loss and decay of radiation belt electrons is identified. Our main conclusions are summarized as follows:

1. Compared to the results for the normal hiss, the unusual hiss causes more efficient pitch angle scattering of $>$ ~50 keV electrons for a broad range of α_{eq}, mainly due to its dominance of wave power at frequencies $<$ 200 Hz. It also results in considerably decreased pitch angle scattering of $<$ 50 keV electrons at most pitch angles and of ~50 keV–2 MeV electrons at high α_{eq}. In addition, the scattering rate bottleneck becomes narrower for 20 keV electrons but broader for hundreds keV electrons with a decreased gradient in $\langle D_{\alpha\alpha}\rangle$ and a transition of minimum $\langle D_{\alpha\alpha}\rangle$ to higher α_{eq}.
2. Pitch angle evolution of tens to hundreds keV electrons due to the unusual hiss scattering behaves distinctly from that due to normal hiss. Scattering by the unusual hiss can slow down the decay of 20 keV electrons but speeds up the loss of ~50–200 keV electrons, showing a maximum decrease by about 1 order of magnitude for ~100 keV electron flux within 2 h. The unusual hiss also causes enhanced pancake distributions of ~50–100 keV electrons but with a narrower top hat feature.
3. Hiss-induced temporal evolution of the electron pitch angle distribution represents a common two-step process that includes a relaxation from the initial condition toward the equilibrium state and a subsequent exponential decay as a whole. Electron lifetimes due to scattering by the unusual low-frequency hiss that only lasted for a couple of hours can be of the order of 1 h for ~50–200 keV electrons.

Our results clearly demonstrate that such unusual (low-frequency) hiss emissions, once present, play an important role in affecting the decay and loss process of energetic electrons, which behaves distinctly from that due to the normal (high-frequency) plasmaspheric hiss and should be carefully incorporated into global modeling of radiation belt electron dynamics, in particular during periods of intense injections. Although the events of enhanced unusual hiss with frequencies well down to tens of hertz are observed quite infrequently in contrast to normal hiss that is commonly confined to a spectrum of 100–2000 Hz, its occurrences are not rare based on the measurements from the Van Allen Probes. The statistical properties of such unusual hiss emissions, their correlations to source electron injection and plasmaspheric configuration, and the relative contribution that they make to the radiation belt electron dynamics is left as future work.

It is also noted that while our study demonstrates that the unusual low-frequency hiss event is important for scattering ~50–200 keV energetic electrons during the short emission duration of a few hours in the dawnside plasmasphere, some other physical processes, including sustained electron injections and electron interactions with chorus waves during the nightside drift trajectory, were also in operation. The effects of these various processes need to be incorporated, besides the pure pitch angle diffusion simulations adopted in this study, into a more sophisticated model to reasonably reproduce observed temporal variations of radiation belt electron distribution. In addition, despite the efficient electron scattering loss of tens to hundreds keV energetic electrons, the short-lived unusual hiss made negligible contribution to the electron flux dropout on 30 September 2012 observed by Van Allen Probes [*Baker et al.*, 2013], which is more likely

attributed to combined effects of magnetopause shadowing, outward radial diffusion, and scattering by whistler mode chorus and electromagnetic ion cyclotron waves.

Acknowledgments
This research was supported by JHU/APL contracts 967399 and 921647 under NASA's prime contract NAS5-01072, NASA grants NNX11AD75G, NNX11AR64G, and NNX13AI61G, and NSF grant AGS-0840178. Work at UCLA was supported by the EMFISIS subaward 1001057397:01 and by the ECT subaward 13-041. We also thank the World Data Center for Geomagnetism, Kyoto for providing *AU* and *AL* indices.

The Editor thanks Mary Hudson and an anonymous reviewer for their assistance in evaluating this paper.

References

Agapitov, O., V. Krasnoselskikh, Y. V. Khotyaintsev, and G. Rolland (2012), Correction to "A statistical study of the propagation characteristics of whistler waves observed by Cluster", *Geophys. Res. Lett.*, *39*, L24102, doi:10.1029/2012GL054320.

Baker, D. N., et al. (2013), A long-lived relativistic electron storage ring embedded in Earth's outer Van Allen belt, *Science*, *340*(6129), 186–190, doi:10.1126/science.1233518.

Blake, J. B., et al. (2013), The Magnetic Electron Ion Spectrometer (MagEIS) instruments aboard the radiation belt storm probes (RBSP) spacecraft, *Space Sci. Rev.*, *179*, 383–421, doi:10.1007/s11214-013-9991-8.

Bortnik, J., L. Chen, W. Li, R. M. Thorne, and R. B. Horne (2011), Modeling the evolution of chorus waves into plasmaspheric hiss, *J. Geophys. Res.*, *116*, A08221, doi:10.1029/2011JA016499.

Chen, L., W. Li, J. Bortnik, and R. M. Thorne (2012), Amplification of whistler mode hiss inside the plasmasphere, *Geophys. Res. Lett.*, *39*, L08111, doi:10.1029/2012GL051488.

Kletzing, C. A., et al. (2013), The Electric and Magnetic Field Instrument Suite and Integrated Science (EMFISIS) on RBSP, *Space Sci. Rev.*, *179*, 127–181, doi:10.1007/s11214-013-9993-6.

Lenchek, A., S. Singer, and R. Wentworth (1961), Geomagnetically trapped electrons from cosmic ray albedo neutrons, *J. Geophys. Res.*, *66*(12), 4027–4046, doi:10.1029/JZ066i012p04027.

Li, W., et al. (2013), An unusual enhancement of low-frequency plasmaspheric hiss in the outer plasmasphere associated with substorm-injected electrons, *Geophys. Res. Lett.*, *40*, 3798–3803, doi:10.1002/grl.50787.

Lyons, L. R., and R. M. Thorne (1973), Equilibrium structure of radiation belt electrons, *J. Geophys. Res.*, *78*(13), 2142–2149.

Mauk, B. H., N. J. Fox, S. G. Kanekal, R. L. Kessel, D. G. Sibeck, and A. Ukhorskiy (2013), Science objectives and rationale for the radiation belt storm probes mission, *Space Sci. Rev.*, *179*, 3–27, doi:10.1007/s11214-012-9908-y.

Meredith, N. P., A. D. Johnstone, S. Szita, R. B. Horne, and R. R. Anderson (1999), "Pancake" electron distributions in the outer radiation belts, *J. Geophys. Res.*, *104*(A6), 12,431–12,444, doi:10.1029/1998JA900083.

Meredith, N. P., R. B. Horne, S. A. Glauert, R. M. Thorne, D. Summers, J. M. Albert, and R. R. Anderson (2006), Energetic outer zone electron loss timescales during low geomagnetic activity, *J. Geophys. Res.*, *111*, A05212, doi:10.1029/2005JA011516.

Meredith, N. P., R. B. Horne, S. A. Glauert, and R. R. Anderson (2007), Slot region electron loss timescales due to plasmaspheric hiss and lightning generated whistlers, *J. Geophys. Res.*, *112*, A08214, doi:10.1029/2006JA012413.

Meredith, N. P., R. B. Horne, S. A. Glauert, D. N. Baker, S. G. Kanekal, and J. M. Albert (2009), Relativistic electron loss timescales in the slot region, *J. Geophys. Res.*, *114*, A03222, doi:10.1029/2008JA013889.

Ni, B., R. M. Thorne, Y. Y. Shprits, and J. Bortnik (2008), Resonant scattering of plasma sheet electrons by whistler-mode chorus: Contribution to diffuse auroral precipitation, *Geophys. Res. Lett.*, *35*, L11106, doi:10.1029/2008GL034032.

Ni, B., J. Bortnik, R. M. Thorne, Q. Ma, and L. Chen (2013), Resonant scattering and resultant pitch angle evolution of relativistic electrons by plasmaspheric hiss, *J. Geophys. Res. Space Physics*, *118*, 7740–7751, doi:10.1002/2013JA019260.

Santolík, O., M. Parrot, L. R. O. Storey, J. S. Picket, and D. A. Gurnett (2001), Propagation analysis of plasmaspheric hiss using Polar PWI measurements, *Geophys. Res. Lett.*, *28*(6), 1127–1130.

Shprits, Y. Y., and B. Ni (2009), Dependence of the quasi-linear scattering rates on the wave normal distribution of chorus waves, *J. Geophys. Res.*, *114*, A11205, doi:10.1029/2009JA014223.

Summers, D., B. Ni, and N. P. Meredith (2007), Timescales for radiation belt electron acceleration and loss due to resonant wave-particle interactions: 2. Evaluation for VLF chorus, ELF hiss, and electromagnetic ion cyclotron waves, *J. Geophys. Res.*, *112*, A04207, doi:10.1029/2006JA011993.

Summers, D., B. Ni, N. P. Meredith, R. B. Horne, R. M. Thorne, M. B. Moldwin, and R. R. Anderson (2008), Electron scattering by whistler-mode ELF hiss in plasmaspheric plumes, *J. Geophys. Res.*, *113*, A04219, doi:10.1029/2007JA012678.

Thorne, R. M., et al. (2013), Evolution and slow decay of an unusual narrow ring of relativistic electrons near $L \sim 3.2$ following the September 2012 magnetic storm, *Geophys. Res. Lett.*, *40*, 3507–3511, doi:10.1002/grl.50627.